Contents

VIP ***The following Communications have been judged by at least two referees to be "very important papers" and will be published online at www.angewandte.org soon:***

*J. Steill, J. Zhao, C.-K. Siu, Y. Ke, U. H. Verkerk, J. Oomens, R. C. Dunbar, A. C. Hopkinson, K. M. Siu**
Structure of the Observable Histidine Radical Cation in the Gas Phase: a Captodative α Radical Ion

*Z. Deng, I. Bald, E. Illenberger, M. A. Huels**
Bond- and Energy-Selective Carbon Abstraction from D-Ribose by Hyperthermal Nitrogen Ions

*J. Spielmann, F. Buch, S. Harder**
Early Main-Group Metal Catalysts for the Hydrogenation of Alkenes with Hydrogen

C. Schäffer, A. Merca, H. Bögge, A. M. Todea, M. L. Kistler, T. Liu, R. Thouvenot, P. Gouzerh, A. Müller**
Unprecedented and Differently Applicable Pentagonal Units in a Dynamic Library: A Keplerate of the Type $\{(W)W_5\}_{12}\{Mo_2\}_{30}$

*T. Seiser, N. Cramer**
Enantioselective C–C Bond Activation of Allenylcyclobutanes: Access to Cyclohexenones with Quaternary Stereogenic Centers

*S. W. Hong, M. Byun, Z. Lin**
Robust Self-Assembly of Highly Ordered Complex Structures by Controlled Evaporation of Confined Microfluids

L. Catala, D. Brinzei, Y. Prado, A. Gloter, O. Stéphan, G. Rogez, T. Mallah**
Core–Multishell Magnetic Coordination Nanoparticles: Towards Multifunctionality at the Nanoscale

*D. Morton, S. Leach, C. Cordier, S. Warriner, A. Nelson**
Synthesis of Natural-Product-Like Molecules with over Eighty Distinct Scaffolds

Books

Asymmetric Phase Transfer Catalysis — Keiji Maruoka — *reviewed by M. Makosza* ——— **8990**

Highlights

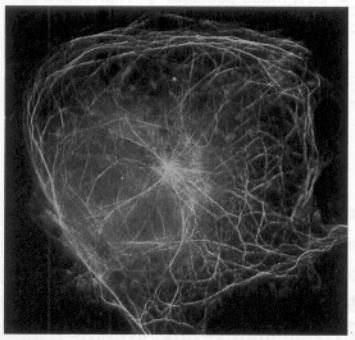

Strike a light! The discovery, isolation, and development of the green fluorescent protein (GFP) and related proteins has revolutionized the specific fluorescence labeling of proteins in cells. GFPs, the subject of the 2008 Nobel Prize in Chemistry, even facilitate the imaging of various parts of cells in different colors (see picture).

Nobel Prize in Chemistry 2008

G. U. Nienhaus* ——— **8992 – 8994**

The Green Fluorescent Protein: A Key Tool to Study Chemical Processes in Living Cells

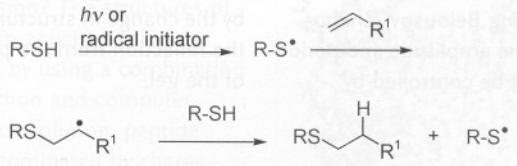

The century-old thiol–ene radical reaction is now being recognized among the ranks of other click-type reactions (see scheme). Recent applications in dendrimer and glycopeptide syntheses demonstrate the efficiency of this process for the assembly of complex molecular systems.

Click Thiol–Ene Chemistry

A. Dondoni* ——— **8995 – 8997**

The Emergence of Thiol–Ene Coupling as a Click Process for Materials and Bioorganic Chemistry

© 2008 Wiley-VCH Verlag GmbH & Co. KGaA, Weinheim

Contents

Reviews

Imaging Methods

P. W. Miller,* N. J. Long, R. Vilar, A. D. Gee ——— **8998 – 9033**

Synthesis of ^{11}C, ^{18}F, ^{15}O, and ^{13}N Radiolabels for Positron Emission Tomography

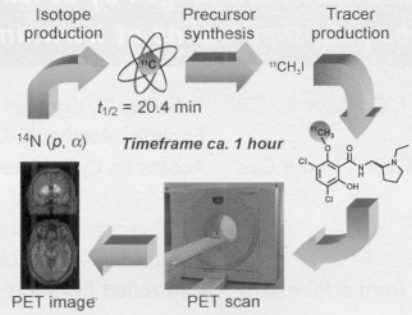

On the fast track: Positron emission tomography relies on the incorporation of a positron-emitting isotope such as ^{11}C, ^{18}F, ^{15}O, or ^{13}N into biologically active compounds. The extremely short half-lives of the isotopes necessitates that the synthesis of the radioactive label is fast and based on simple prepartive methods (see picture).

Communications

Telomerase

H. Yu, D. Zhang, X. Gu, D. Miyoshi, N. Sugimoto* ——— **9034 – 9038**

Regulation of Telomerase Activity by the Thermodynamic Stability of a DNA·RNA Hybrid

Slide or stick: The thermodynamic stability of a hybrid composed of substrate DNA and template RNA derived from telomerase was investigated under dilute and molecular-crowding conditions. Destabilization of the hybrid by cosolutes of low molecular weight (MW) leads to an easier sliding of telomerase along the telomeric DNA (see picture). In contrast, telomerase tends to stick to the telomeric DNA when the hybrid is stabilized by high-MW cosolutes.

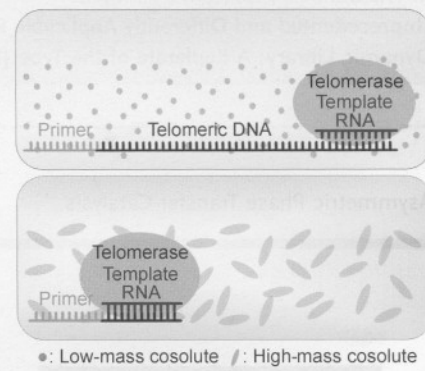

Polymer Gels

S. Shinohara, T. Seki, T. Sakai, R. Yoshida, Y. Takeoka* ——— **9039 – 9043**

Photoregulated Wormlike Motion of a Gel

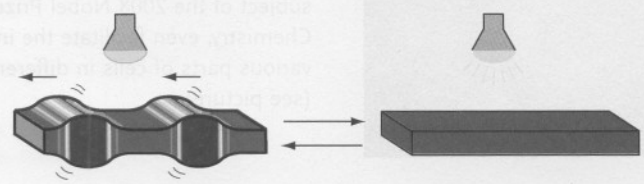

Global worming: A periodically ordered mesoporous gel demonstrates photoregulated peristaltic motion induced by a nonlinear oscillating Belousov–Zhabotinsky reaction. The amplitude and period of the motion can be controlled by adjusting the intensity of visible light irradiation (see picture). Peristaltic motion of the gel surface can be observed by the change in structural color based on the reflection from the photonic bandgap of the gel.

For the USA and Canada:
ANGEWANDTE CHEMIE International Edition (ISSN 1433-7851) is published weekly by Wiley-VCH, PO Box 191161, 69451 Weinheim, Germany. Air freight and mailing in the USA by Publications Expediting Inc., 200 Meacham Ave., Elmont, NY 11003. Periodicals postage paid at Jamaica, NY 11431. US POSTMASTER: send address changes to *Angewandte Chemie*, Wiley-VCH, 111 River Street, Hoboken, NJ 07030. Annual subscription price for institutions: US$ 7225/6568 (valid for print and electronic / print or electronic delivery); for individuals who are personal members of a national chemical society prices are available on request. Postage and handling charges included. All prices are subject to local VAT/sales tax.

© 2008 Wiley-VCH Verlag GmbH & Co. KGaA, Weinheim

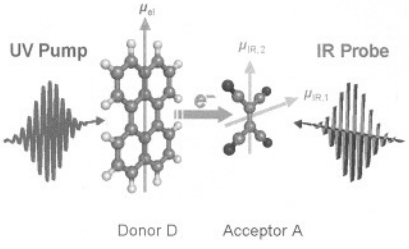

Polarization-sensitive ultrafast infrared measurements on photoinduced electron transfer in donor–acceptor pairs in polar acetonitrile show distinct contributions from loose and tight ion pairs. Highly anisotropic signals from tight ion pairs reveal the importance of mutual orientation of the reactants (see picture) and thus the need to refine theoretical models based on spherical species that solely involve reaction distances.

Bimolecular Electron Transfer

O. F. Mohammed, K. Adamczyk, N. Banerji, J. Dreyer, B. Lang, E. T. J. Nibbering,* E. Vauthey* ——— **9044 – 9048**

Direct Femtosecond Observation of Tight and Loose Ion Pairs upon Photoinduced Bimolecular Electron Transfer

Transfer request: A self-assembled supramolecular charge-transfer complex of 1-(11-oxo-11-pyren-1-ylmethoxy)undecyl)-pyridinium bromide (PYR) and ethane-1,2-diyl bis(3,5-dinitrobenzoate) (DNB) is shown to form vesicular aggregates in aqueous solution, in contrast to the tubular aggregates of pure PYR (see picture). A curvature-dependent mechanism for this change is proposed.

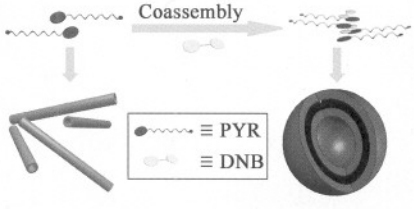

Controlled Self-Assembly

C. Wang, S. C. Yin, S. L. Chen, H. P. Xu, Z. Q. Wang, X. Zhang* ——— **9049 – 9052**

Controlled Self-Assembly Manipulated by Charge-Transfer Interactions: From Tubes to Vesicles

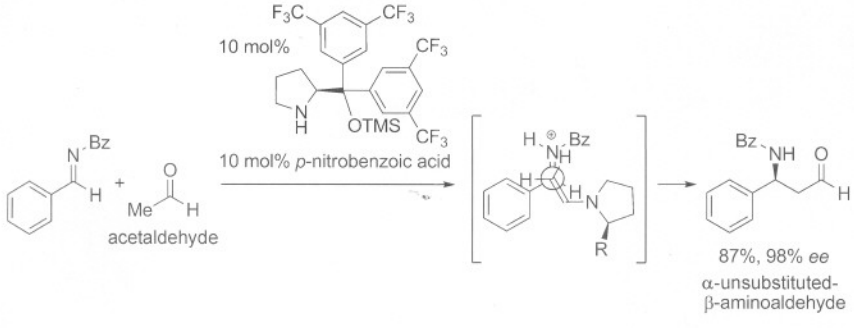

Asymmetric Catalysis

Y. Hayashi,* T. Okano, T. Itoh, T. Urushima, H. Ishikawa, T. Uchimaru* ——— **9053 – 9058**

Direct Organocatalytic Mannich Reaction of Acetaldehyde: An Improved Catalyst and Mechanistic Insight from a Computational Study

A chiral diaryl prolinol silyl ether organocatalyst with an acid is used for the direct catalytic asymmetric Mannich reaction of acetaldehyde and imines. *N*-Benzoyl-, *N*-*tert*-butoxycarbonyl-, and *N*-toluene-4-sulfonylimines can be employed to produce synthetically useful β-amino aldehydes in good yields and with excellent enantioselectivity (see scheme). The reaction mechanism was investigated quantum-mechanically.

What's the attraction? The structures of three dipeptides in aqueous solutions were investigated by using a combination of neutron diffraction and computer simulation. In each solution, peptide association was dominated by charge–charge rather than hydrophobic interactions (see the representative snapshot of the peptide/water box for glycyl-L-alanine; the water molecules are depicted by red crosses.)

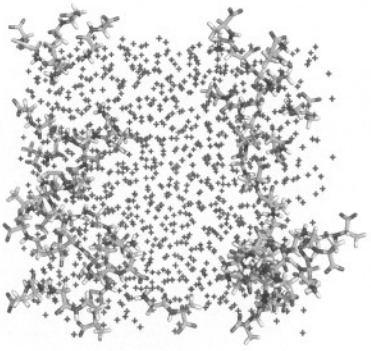

Peptide Clusters

S. E. McLain,* A. K. Soper, I. Daidone, J. C. Smith, A. Watts ——— **9059 – 9062**

Charge-Based Interactions between Peptides Observed as the Dominant Force for Association in Aqueous Solution

© 2008 Wiley-VCH Verlag GmbH & Co. KGaA, Weinheim

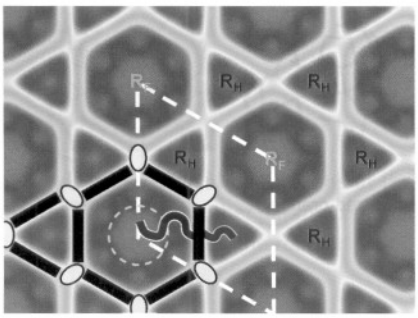

No place like kagome: A quaternary amphiphile displays a novel complex liquid-crystalline phase formed by a periodic array combining triangular and hexagonal cylinders, filled with hydrocarbon and fluorinated chains, respectively. This leads to a fluid nanoscale multicompartment structure with kagome geometry. The thickness of the intercompartment walls is equal to the width of the π-conjugated rods (shown as black lines).

Liquid Crystals

B. Glettner, F. Liu, X. B. Zeng, M. Prehm, U. Baumeister, M. Walker, M. A. Bates, P. Boesecke, G. Ungar,* C. Tschierske* ——— **9063 – 9066**

Liquid-Crystalline Kagome

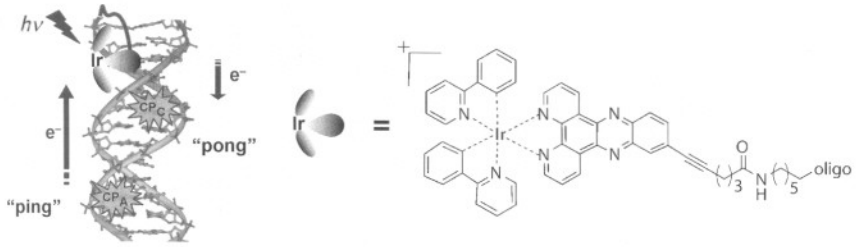

Either way: An Ir^{III} complex strongly coupled to a DNA base stack can inject a hole or an electron in DNA upon irradiation (see picture). With strands containing the modified bases ^{CP}A and $^{CP}C/^{Br}U$, which serve as oxidative and reductive probes, respectively, photolysis of Ir–DNA conjugates leads to a "ping-pong" electron transfer, with both hole and electron migration.

Electron Transfer in DNA

B. Elias, J. C. Genereux, J. K. Barton* ——— **9067 – 9070**

Ping-Pong Electron Transfer through DNA

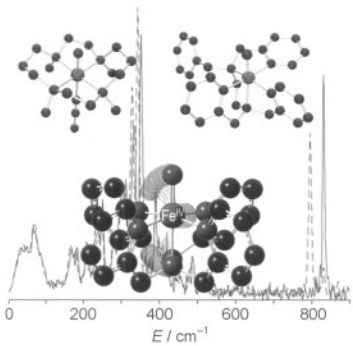

In the swing of things: Fe^{IV}=O biomimetic model complexes (see picture, Fe green, O red, N blue, C black) have been characterized using nuclear vibrational resonance spectroscopy. Systematic trends in the low-energy region reflect equatorial and axial bonding differences that relate to differences in reactivity. These trends have been computationally extended to predict the spectra of putative Fe^{IV}=O intermediates in non-heme iron enzymes.

Bioinorganic Chemistry

C. B. Bell, III, S. D. Wong, Y. Xiao, E. J. Klinker, A. L. Tenderholt, M. C. Smith, J.-U. Rohde, L. Que, Jr., S. P. Cramer, E. I. Solomon* ——— **9071 – 9074**

A Combined NRVS and DFT Study of Fe^{IV}=O Model Complexes: A Diagnostic Method for the Elucidation of Non-Heme Iron Enzyme Intermediates

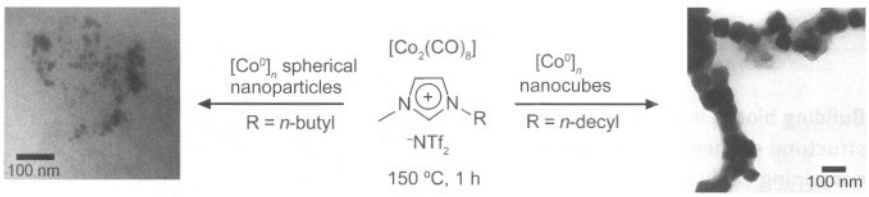

Cubes and spheres: The simple thermal decomposition of $[Co_2(CO)_8]$ dispersed in 1-alkyl-3-methyl imidazolium ionic liquids can preferentially generate either ligand-free cobalt nanocubes or spherical nanoparticles, depending on the type of ionic liquid and the decomposition time. These nanostructures can act as selective catalysts in the Fischer–Tropsch synthesis.

Nanostructures

M. Scariot, D. O. Silva, J. D. Scholten, G. Machado, S. R. Teixeira, M. A. Novak, G. Ebeling, J. Dupont* ——— **9075 – 9078**

Cobalt Nanocubes in Ionic Liquids: Synthesis and Properties

© 2008 Wiley-VCH Verlag GmbH & Co. KGaA, Weinheim

Contents

Mg–Mg Bonds

S. P. Green, C. Jones,*
A. Stasch* _____ **9079 – 9083**

Stable Adducts of a Dimeric Magnesium(I) Compound

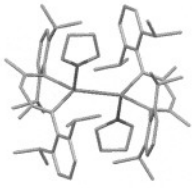

A bit of a stretch! A series of stable Lewis base adducts of a dimeric magnesium(I) complex has been prepared and shown to possess exceptionally long Mg–Mg bonds. Theoretical studies on model compounds suggest the elongations of these bonds are low-energy processes. The structures of the magnesium(I) adducts are compared with those of related magnesium(II) hydride complexes (see picture; Mg pink, N blue, O red, H green).

Peptide Chemistry

R. A. Himes, G. Y. Park, G. S. Siluvai, N. J. Blackburn, K. D. Karlin* _____ **9084 – 9087**

Structural Studies of Copper(I) Complexes of Amyloid-β Peptide Fragments: Formation of Two-Coordinate Bis(histidine) Complexes

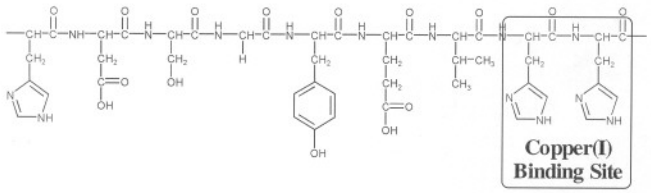

The beta bind: Copper(I) binds to amyloid β-peptide fragments (see structure) as a stable bis(histidine), two-coordinate, near-linear complex, even in the presence of potential additional ligands. As has been proposed or assumed in other studies, the copper(I)–peptide complexes react with dioxygen to form the reactive oxygen species H_2O_2, without the need for a third histidine ligand to promote the chemistry.

Stereocontrolled Polymerization

M. Florczak, A. Duda* _____ **9088 – 9091**

Effect of the Configuration of the Active Center on Comonomer Reactivities: The Case of ε-Caprolactone/ L,L-Lactide Copolymerization

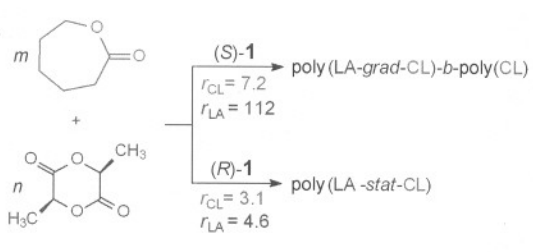

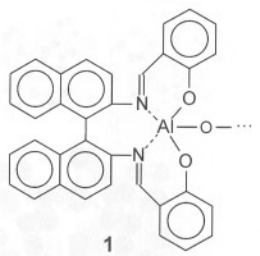

Pick your polymer: The reactivity ratios, *r*, of the comonomers can be controlled by the configuration of the active species in the copolymerization of ε-caprolactone (CL) and L,L-lactide (LA; see scheme). Thus, by varying the configuration of the initiator, a broad spectrum of copolymers with different microstructures, from gradient to more random, can be prepared in a controlled way.

Zeolites

B. B. Schaack, W. Schrader, F. Schüth* _____ **9092 – 9095**

Detection of Structural Elements of Different Zeolites in Nucleating Solutions by Electrospray Ionization Mass Spectrometry

Building blocks in solution: Characteristic structural elements of the germanium-containing zeolites ZSM-5, polymorph C of zeolite Beta, and zeolite A (see picture) are identified in solution immediately before nucleation. The conditions of the reaction direct the polycondensation of silicate towards specific structures at the solution stage.

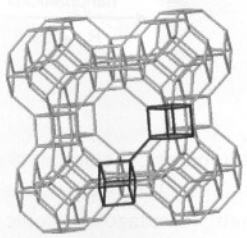

© 2008 Wiley-VCH Verlag GmbH & Co. KGaA, Weinheim

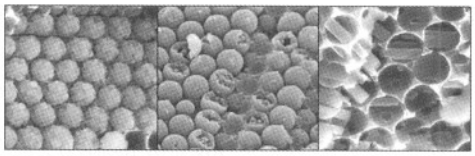

Cooking in a small pot: Uniform zeolite particles (see picture) can be prepared in high yield by hydrothermal syntheses within the confinement of inverse-opal carbon reactors. The product morphology depends on interfacial interactions at the reactor walls and on other parameters that can be engineered into the reactor process.

Zeolites

W. C. Yoo, S. Kumar, Z. Wang, N. S. Ergang, W. Fan, G. N. Karanikolos, A. V. McCormick, R. L. Penn, M. Tsapatsis, A. Stein* _____ 9096 – 9099

Nanoscale Reactor Engineering: Hydrothermal Synthesis of Uniform Zeolite Particles in Massively Parallel Reaction Chambers

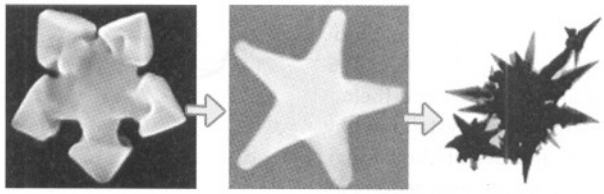

Star performance: The shape and surface structure of star-shaped gold nanoparticles (NPs) bounded by (331) and vicinal high-index facets, now synthesized for the first time, can be tuned by varying the water content in the deep eutetic solvent. The results confirm that star-shaped Au NPs exhibit superior activity for electrocatalytic reduction of H_2O_2. The ability to tune the shape offers insight into structure–functionality relationships.

Nanostructures

H. G. Liao, Y. X. Jiang,* Z. Y. Zhou, S. P. Chen, S. G. Sun* _____ 9100 – 9103

Shape-Controlled Synthesis of Gold Nanoparticles in Deep Eutectic Solvents for Studies of Structure–Functionality Relationships in Electrocatalysis

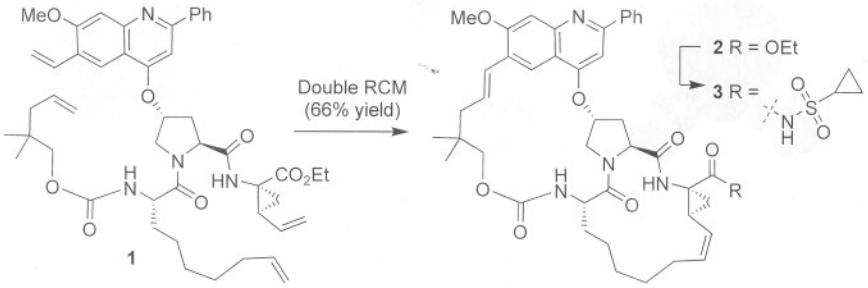

Double time: The bismacrocycle **2** was prepared from **1** by a selective double ring-closing metathesis (RCM) reaction to form the 18- and 15-membered rings simultaneously. Derivative **3** shows excellent potency against NS3/4a protease.

Ring-Closing Metathesis

J. A. McCauley,* M. T. Rudd, K. T. Nguyen, C. J. McIntyre, J. J. Romano, K. J. Bush, S. L. Varga, C. W. Ross, III, S. S. Carroll, J. DiMuzio, M. W. Stahlhut, D. B. Olsen, T. A. Lyle, J. P. Vacca, N. J. Liverton _____ 9104 – 9107

Bismacrocyclic Inhibitors of Hepatitis C NS3/4a Protease

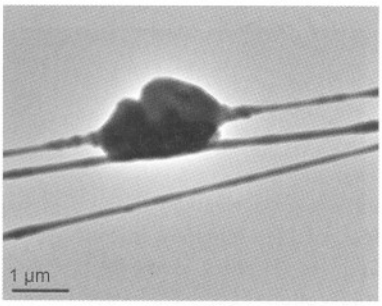

Spinning a web: The electrospinning of cyclodextrin (CD) pseudopolyrotaxane, α-CD–PEG-IC (PEG = poly(ethylene glycol), IC = inclusion complex), nanofibers using poly(ethylene oxide) as a carrier polymer matrix has been achieved (see picture) without destruction of the pseudopolyrotaxane structure. This opens up a variety of possibilities for the development of multifunctional nanofibers containing CD pseudopolyrotaxanes and/or CD inclusion complexes.

Inclusion Compounds

T. Uyar,* P. Kingshott, F. Besenbacher _____ 9108 – 9111

Electrospinning of Cyclodextrin–Pseudopolyrotaxane Nanofibers

© 2008 Wiley-VCH Verlag GmbH & Co. KGaA, Weinheim

Contents

Nickel(II) Complexes

H. Fan, B. C. Fullmer, M. Pink, K. G. Caulton* ——— **9112–9114**

[Ni{N(SiMe$_2$CH$_2$P*t*Bu$_2$)$_2$}]$^+$: Direct Observation of Transannular Si–C(sp^3) Bond Coordination

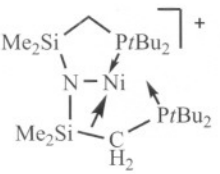

How low can you go? The title [(PNP)Ni]$^+$ complex is not a T-shaped d^8 cation. Rather, it has an electrophilic Ni^{II} center bound to one of the Si–C bonds, stretching it by nearly 0.2 Å. This example shows that there are limits to how unsaturated Ni^{II} centers can be.

Metal–Metal Interactions

T. Nguyen, W. A. Merrill, C. Ni, H. Lei, J. C. Fettinger, B. D. Ellis, G. J. Long, M. Brynda, P. P. Power* ——— **9115–9117**

Synthesis and Characterization of the Metal(I) Dimers [Ar′MMAr′]: Comparisons with Quintuple-Bonded [Ar′CrCrAr′]

Cobalt together: The iron and cobalt analogues of the quintuple-bonded chromium species [Ar′CrCrAr′] (Ar′ = C$_6$H$_3$-2,6-(2,6-*i*Pr$_2$C$_6$H$_3$)$_2$) are described and their structures investigated by crystallography, magnetic studies, and density functional calculations. Metal-η^6-aryl interactions in [Ar′FeFeAr′] and [Ar′CoCoAr′] are stronger than those detected in [Ar′CrCrAr′], whereas metal–metal bonding is much weaker.

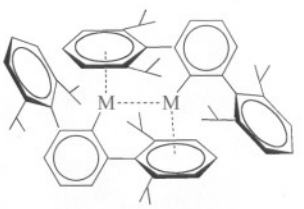

Coordinated Ketyl Radicals

C. C. L. Thum, G. N. Khairallah, R. A. J. O'Hair* ——— **9118–9121**

Gas-Phase Formation of the Gomberg–Bachmann Magnesium Ketyl

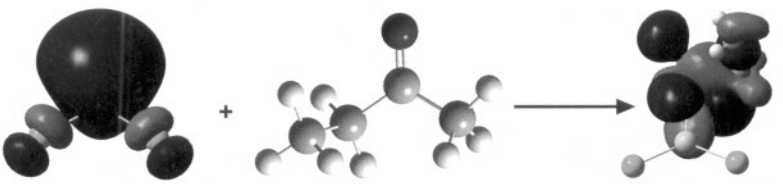

$MgCl_2^{\bullet-}$, synthesized in the gas phase, reacts with ketones to produce the corresponding Gomberg–Bachmann magnesium ketyl radical anion, which further leads to a magnesium enolate through β scission. DFT calculations support the reactions observed and reveal that the singly occupied molecular orbital changes from metal-based in the reactant to ligand-based in the product (see picture).

Asymmetric Catalysis

H. Hénon, M. Mauduit, A. Alexakis* ——— **9122–9124**

Regiodivergent 1,4 versus 1,6 Asymmetric Copper-Catalyzed Conjugate Addition

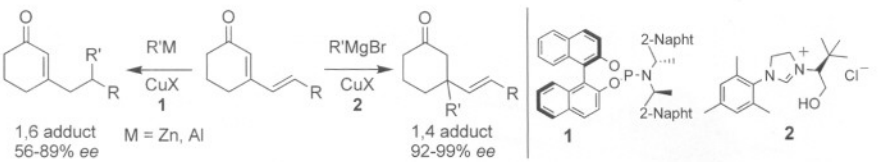

Metal matters: A highly regiodivergent copper-catalyzed asymmetric conjugate addition to α,β and γ,δ Michael acceptors is described. Zinc and aluminum reagents afford the 1,6 adduct with good to moderate enantioselectivity in the presence of ligand **1** (see scheme). In contrast, Grignard reagents used with hydroxy imidazolium ligand **2** afforded the 1,4 adduct with excellent *ee* values.

© 2008 Wiley-VCH Verlag GmbH & Co. KGaA, Weinheim

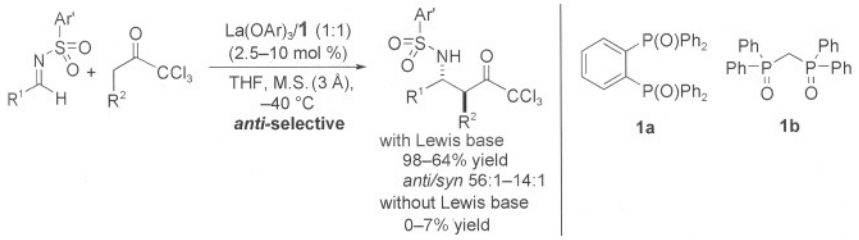

Dynamic Duo: A Lewis basic bidentate phosphine oxide was effective for activating and modulating the properties of Brønsted basic lanthanum aryl oxides. The Lewis base **1**/lanthanum aryl oxide system was suitable for *anti*-selective Mannich-type reactions of trichloromethyl ketones (see scheme), affording unique building blocks for azetidine-2-carboxylic acids as well as β-amino acids.

Synthetic Methods

H. Morimoto, T. Yoshino, T. Yukawa, G. Lu, S. Matsunaga,* M. Shibasaki* _____ 9125–9129

Lewis Base Assisted Brønsted Base Catalysis: Bidentate Phosphine Oxides as Activators and Modulators of Brønsted Basic Lanthanum–Aryloxides

Radically shortened: In the propagation step of the title reaction, the cyclohexadienyl radical intermediate is oxidized by an arenediazonium ion to give the biaryl product (see scheme) while simultaneously a new aryl radical and nitrogen are formed.

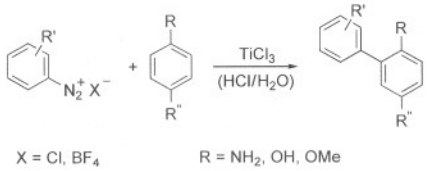

Biaryls

A. Wetzel, V. Ehrhardt, M. R. Heinrich* _____ 9130–9133

Synthesis of Amino- and Hydroxybiphenyls by Radical Chain Reaction of Arenediazonium Salts

Final proof of the complete structures of thuggacins A–C was gained by a highly convergent and flexible total synthesis. Notable features include a substrate-controlled, titanium-mediated aldol reaction, a cross-metathesis approach for converting terminal alkenes into the corresponding vinyl iodides, and the cross-coupling of a complex vinyl iodide and terminal alkyne in the Sonogashira reaction.

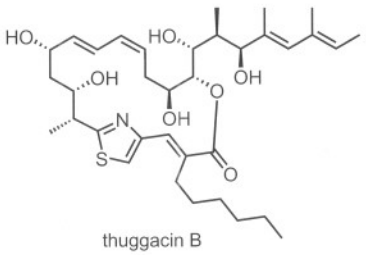

Natural Product Synthesis

M. Bock, R. Dehn, A. Kirschning* _____ 9134–9137

Total Synthesis of Thuggacin B

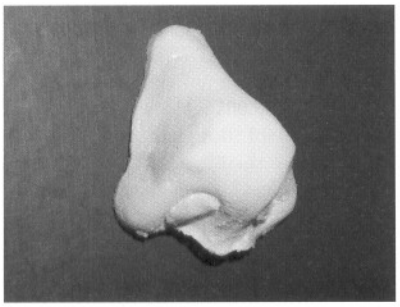

Need a new nose? Biocompatible, highly porous monolithic scaffolds have been prepared by electron-beam-initiated free-radical polymerization and ring-opening metathesis polymerization. These scaffolds can be used for the in vitro construction of equivalents to bone and fatty tissue. Thus, autologous stem cells have been differentiated into both lipoblasts and osteocytes.

Tissue Engineering

A. Löber, A. Verch, B. Schlemmer, S. Höfer, B. Frerich,* M. R. Buchmeiser* _____ 9138–9141

Monolithic Polymers for Cell Cultivation, Differentiation, and Tissue Engineering

© 2008 Wiley-VCH Verlag GmbH & Co. KGaA, Weinheim

Contents

Reversible CO Coordination

D. Benito-Garagorri, M. Puchberger, K. Mereiter, K. Kirchner* — **9142 – 9145**

Stereospecific and Reversible CO Binding at Iron Pincer Complexes

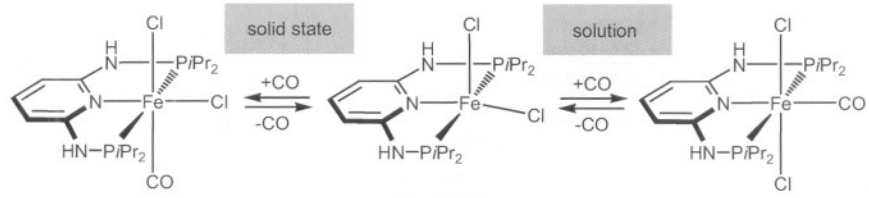

An opening for CO: An iron PNP pincer complex self-assembles in the solid state through intermolecular Fe–Cl···H–N hydrogen bonds to form a 3D supramolecular network. This compound reacts readily with gaseous CO in the solid state and in solution to stereospecifically give the octahedral complexes *cis*- and *trans*-[Fe(PNP-*i*Pr)(CO)(Cl)$_2$], respectively. In the solid-state process the supramolecular connectivities between individual molecules are maintained without loss of crystallinity.

Cluster Compounds

T. Cadenbach, C. Gemel, R. A. Fischer* — **9146 – 9149**

Molecular Cut-Outs of Mo/Zn Hume–Rothery Phases: Synthesis and Structure of [{Mo(CO)$_4$}$_4$(Zn)$_6$(μ-ZnCp*)$_4$]

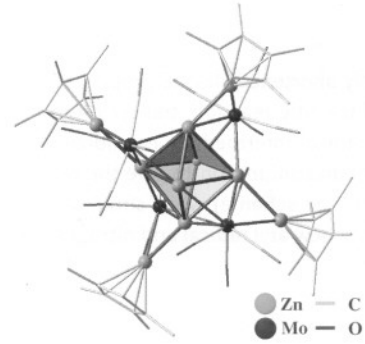

Zinc in the middle: The reaction of [Mo(GaCp*)$_2$(CO)$_4$] and Zn(CH$_3$)$_2$ results in the cluster [{Mo(CO)$_4$}$_4$(Zn)$_6$(μ-ZnCp*)$_4$] (see picture), the first metalloid cluster with naked zinc atoms as cluster elements. This complex indeed represents a molecular cut-out of a Mo/Zn alloy, which is not only substantiated by similar interatomic distances but by direct comparison of coordination environments of the metal atoms.

Cluster Compounds

T. Cadenbach, T. Bollermann, C. Gemel, I. Fernandez, M. von Hopffgarten, G. Frenking,* R. A. Fischer* **9150 – 9154**

Twelve One-Electron Ligands Coordinating One Metal Center: Structure and Bonding of [Mo(ZnCH$_3$)$_9$(ZnCp*)$_3$]

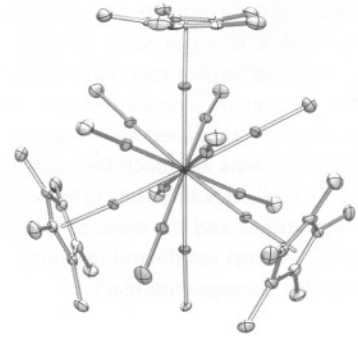

Surrounded by zinc: The reaction of [Mo(GaCp*)$_6$] and Zn(CH$_3$)$_2$ zinc yields the exceptionally high-coordinate title compound (see picture; Mo red, Zn green, C gray). Quantum chemical analysis reveals a unique bonding situation best described as a perfectly sd^5 hybridized molybdenum atom with 12 valence electrons engaged in Mo–Zn bonding. Another six electrons are delocalized over the Zn cage, evoking only weak Zn–Zn interactions.

Supporting information is available on www.angewandte.org (see article for access details).

A video clip is available as Supporting Information on www.angewandte.org (see article for access details).

© 2008 Wiley-VCH Verlag GmbH & Co. KGaA, Weinheim

Looking for outstanding employees?

Do you need another expert for your excellent team?
... Chemists, PhD Students, Managers, Professors, Sales Representatives...

Place an advert in the printed version and have it made available online for 1 month, free of charge!

Angewandte Chemie International Edition
Advertising Sales Department: Marion Schulz
Phone: 0 62 01 - 60 65 65
Fax: 0 62 01 - 60 65 50
E-Mail: MSchulz@wiley-vch.de

Service

Spotlights Angewandte's Sister Journals ____ *8988 – 8989*

Keywords ____ *9156*

Authors ____ *9157*

Preview ____ *9159*

Corrigendum

In this Communication the Table of Contents graphic is incorrect. The Editorial Office apologizes for this error. The correct graphic is shown.

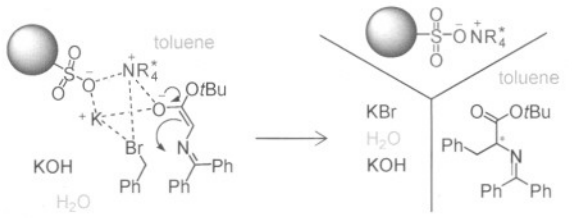

An Immobilization Method of Chiral Quaternary Ammonium Salts onto Polymer Supports

Y. Arakawa, N. Haraguchi, S. Itsuno* ____ **8232–8235**

Angew. Chem. Int. Ed. **2008**, *47*

DOI 10.1002/anie.200802800

Apology

The authors of this Communication inadvertently omitted citation of their own prior work discussing a specific fluorescent probe for 8-oxoguanosine. These reports should be included as reference [11f]. The authors apologize for their oversight.

[11] a) K.-Y. Lin, M. D. Matteucci, *J. Am. Chem. Soc.* **1998**, *120*, 8531 – 8532; b) W. M. Flanagan, J. J. Wolf, P. Olson, D. Grant, K.-Y. Lin, R. W. Wagner, M. D. Matteucci, *Proc. Natl. Acad. Sci. USA* **1999**, *96*, 3513 – 3518; c) M. A. Maier, J. M. Leeds, G. Balow, R. H. Springer, R. Bharadwaj, M. Manoharan, *Biochemistry* **2002**, *41*, 1323 – 1327; d) C. J. Wilds, M. A. Maier, V. Tereshko, M. Manoharan, M. Egli, *Angew. Chem.* **2002**, *114*, 123 – 125; *Angew. Chem. Int. Ed.* **2002**, *41*, 115 – 117; e) S. C. Holmes, A. A. Arzumanov, M. J. Gait, *Nucleic Acids Res.* **2003**, *31*, 2759 – 2768; f) for preliminary studies on G-clamp derivatives as a fluorescent probe for 8-oxoguanosine, see: O. Nakagawa, S. Ono, A. Tsujimoto, Z. Li, S. Sasaki, *Nucleic Acids Symp. Ser.* **2006**, *50*, 21-22, and O. Nakagawa, S. Ono, A. Tsujimoto, Z. Li, S. Sasaki, *Nucleosides Nucleotides Nucleic Acids* **2007**, *26*, 645-649.

Specific Fluorescent Probe for 8-Oxoguanosine

O. Nakagawa, S. Ono, Z. Li, A. Tsujimoto, S. Sasaki* ____ **4500–4503**

Angew. Chem. Int. Ed. **2007**, *46*

DOI 10.1002/anie.200700671

© 2008 Wiley-VCH Verlag GmbH & Co. KGaA, Weinheim